

Supplementary Materials for

Batch growth of wafer scale nanocrystalline NbSe₂ film for surface-enhanced Raman spectroscopy

Huihui Lin^{1,2,#,*}, Yiwen Li^{2,#}, Yuxin Li^{3,#}, Meng-Xuan Li⁴, Luyan Wu^{5,*}, Zhaolong Chen^{6,*} and Jing Li^{4,*}

¹Institute of Sustainability for Chemicals, Energy and Environment (ISCE2), Agency for Science, Technology and Research (A*STAR), Singapore 627833, Singapore;

²National Laboratory of Solid State Microstructures, School of Physics, Nanjing University, Nanjing 210093, China;

³State Key Laboratory of Nuclear Physics and Technology, Center for Applied Physics and Technology, Peking University, Beijing 100871, China;

⁴Key Laboratory of Bio-inspired Smart Interfacial Science and Technology of Ministry of Education, School of Chemistry, Beihang University, Beijing 100191, China;

⁵State Key Laboratory for Organic Electronics and Information Displays, Jiangsu Key Laboratory for Biosensors, Institute of Advanced Materials (IAM), Jiangsu National Synergetic Innovation Center for Advanced Materials (SICAM), School of Materials Science and Engineering, Nanjing University of Posts and Telecommunications, Nanjing 210023, China;

⁶Guangdong Provincial Key Laboratory of Nano-Micro Materials Research, School of Advanced Materials, Peking University Shenzhen Graduate School, Peking University, Shenzhen 518055, China

#Equally contributed to this work.

*Corresponding author (e-mails: linhh@isce2.a-star.edu.sg; iamlywu@njupt.edu.cn; chenzhaolong@pku.edu.cn; chmlj@buaa.edu.cn)

This Supplementary Information includes the following sections:

- S1. The roughness of Nb film sputtered on SiO₂/Si.
- S2. Substrate-dependent crystalline quality of as-sputtered Nb films.
- S3. Raman spectra of NC-NbSe₂ film with perpendicular polarization.
- S4. AFM image and the corresponding height profile of C-NbSe₂ films directly grown on sapphire.
- S5. Substrate-dependent transport property of as-grown NbSe₂ films.
- S6. Atomic model structures of GBs of NC-NbSe₂.
- S7. Origin of the SERS effect of NC-NbSe₂.
- S8. The SERS performance evaluation of NC-NbSe₂ film for different dyes.
- S9. SERS effect of as-grown NC-NbSe₂ film as a function of dye concentrations.
- S10. Air-stable SERS effect of as-grown NC-NbSe₂ film.
- S11. Instability of electrochemically exfoliated NbSe₂ flakes.
- S12. Origin of instability in electrochemically exfoliated NbSe₂ flakes.
- S13. Pristine NbSe₂ flakes in air.
- S14. NbSe₂ flakes with points defect in air.
- S15. Stable SERS effect of NC-NbSe₂ film.
- S16. Homogenous SERS performance of as-grown 4-inch NC-NbSe₂ film.

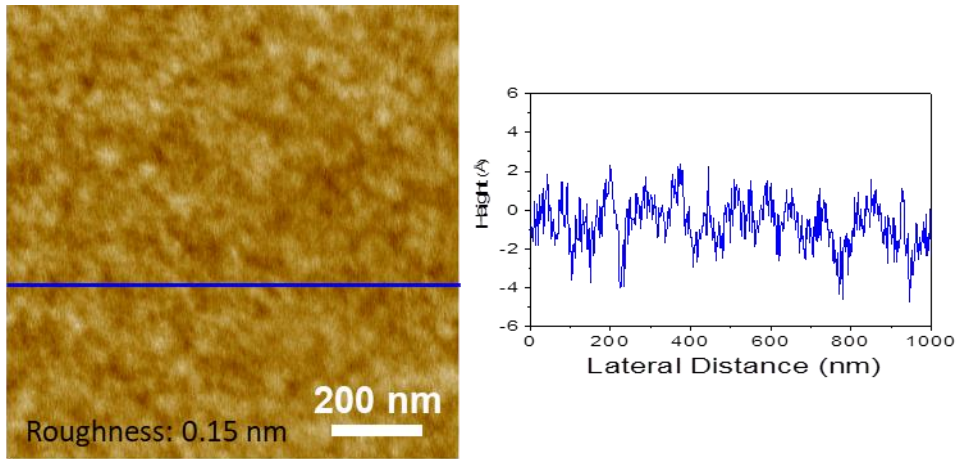


Figure S1. The roughness of Nb film sputtered on SiO₂/Si. AFM image (Left) and the corresponding height profile of a nanocrystalline Nb film sputtered on SiO₂/Si (Right) at room temperature.

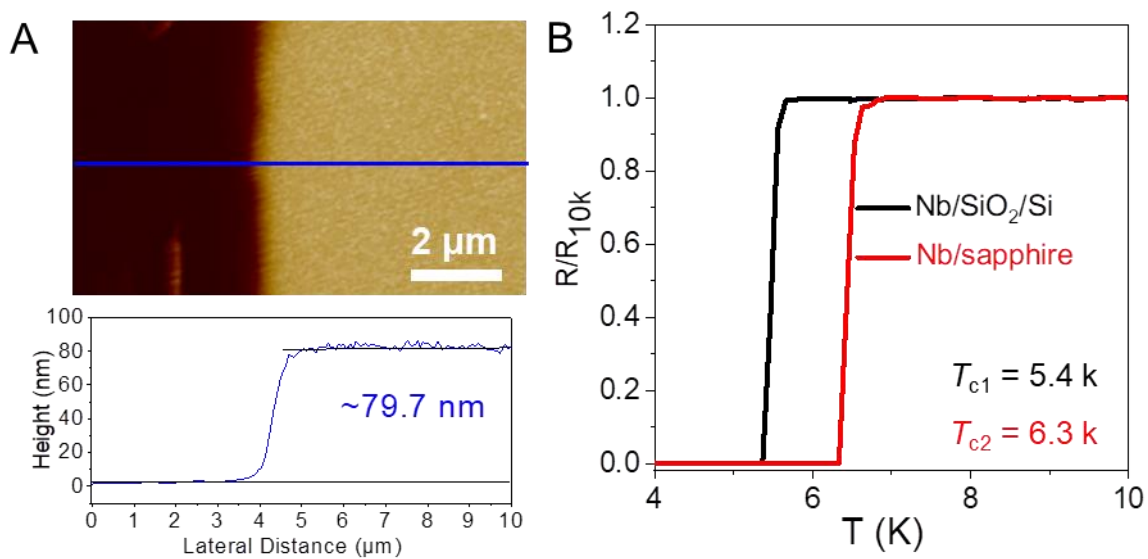


Figure S2. Substrate-dependent crystalline quality of as-sputtered Nb films at the same sputtering conditions. (A) AFM image and the corresponding height profile of an as-sputtered Nb film. (B) Superconductivity of the Nb films on SiO₂/Si and sapphire under the same sputtering conditions (e.g., sputtered at room temperature). Note: The superconducting transition critical temperature (T_c): the temperature at which the sheet resistance drops to 10% of its normal state.

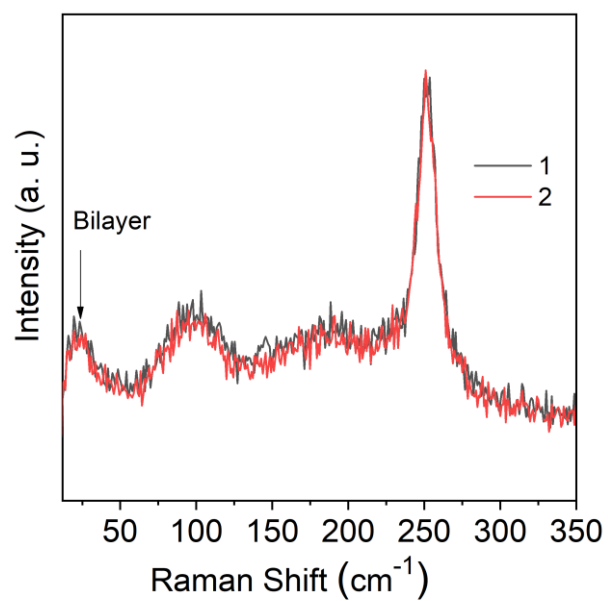


Figure S3. Raman spectra of NC-NbSe₂ film with perpendicular polarization.

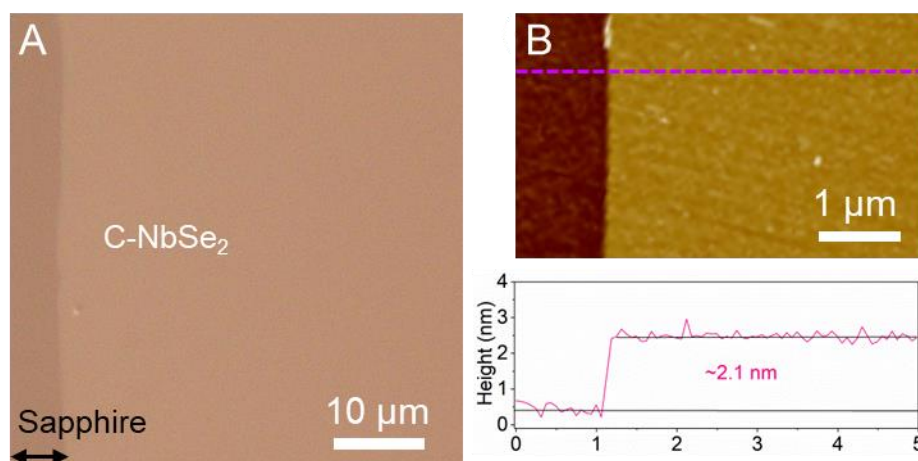


Figure S4. Morphology characterization of C-NbSe₂ films directly grown on sapphire. (A) optical microscopic image of as-grown C-NbSe₂ film on sapphire substrates. (B) AFM image and the corresponding height profile of C-NbSe₂ films directly grown on sapphire.

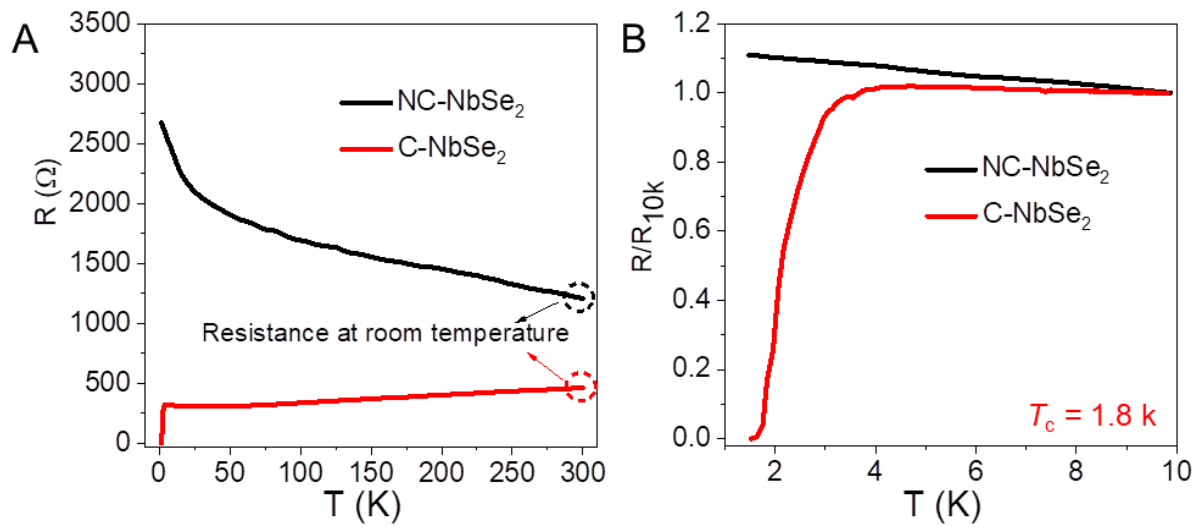


Figure S5. Substrate-dependent transport property of as-grown NbSe₂ films the same mild growth conditions. The temperature dependence resistance of NbSe₂ films on SiO₂/Si and sapphire (referred as NC-NbSe₂, NC-NbSe₂, respectively) at a mild growth temperature (550 °C). The resistance of NbSe₂ films on SiO₂/Si and sapphire at room temperature are marked by a black dotted circle frame and a red dotted circle frame in (A), respectively. The resistance in (B) is normalized by the resistance at the temperature of 10 K (the normal state of Superconducting NbSe₂).

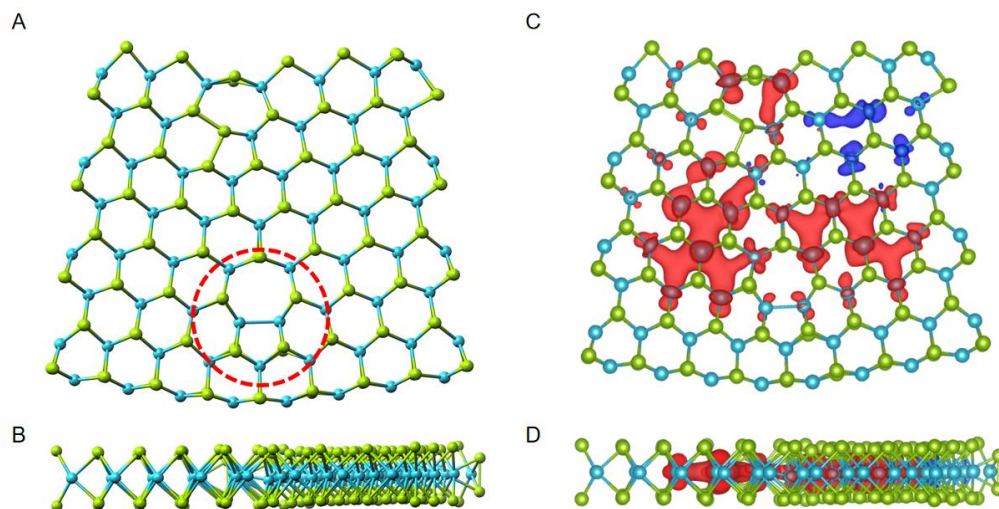


Figure S6. Atomic model structures of GBs of NC-NbSe₂. (A-B) Atomic model structures of GBs of NC-NbSe₂. (C-D) Spin density of GBs of NC-NbSe₂ (Spin up: red, spin down: blue, isosurface= ± 0.002).

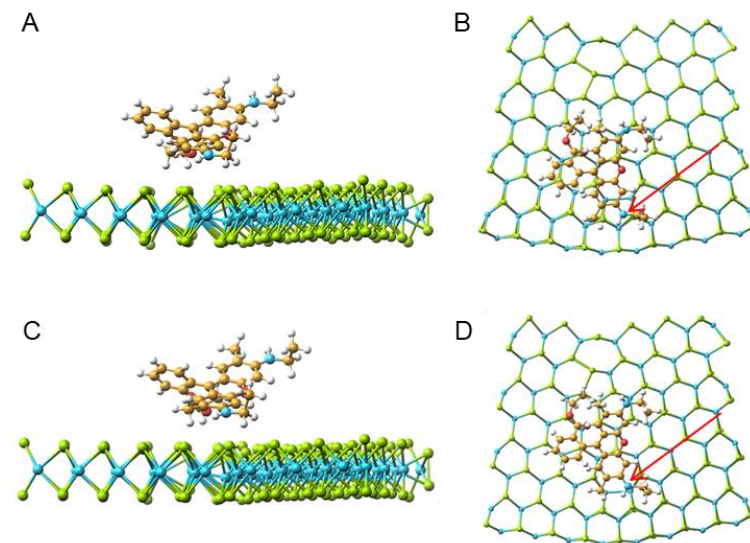


Figure S7. Origin of the SERS effect of NC-NbSe₂. Side-view and top-view of R6G molecules adsorbed on the NC-NbSe₂ surface, illustrating the adsorption configurations on (A, B) pentagonal rings, (C, D) heptagonal rings.

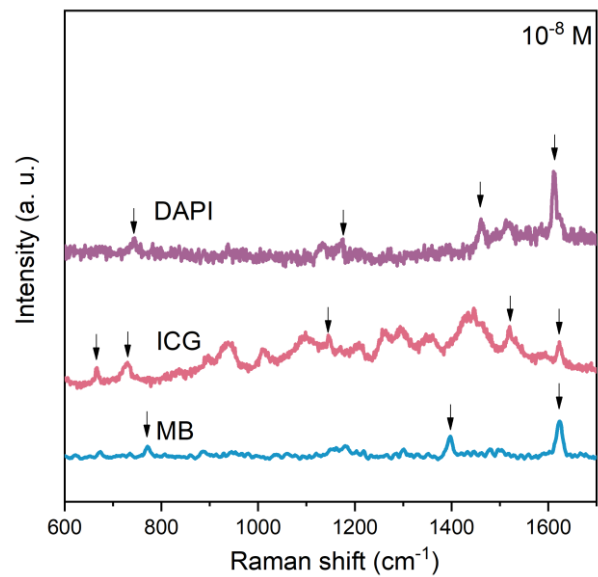


Figure S8. The SERS performance evaluation of NC-NbSe₂ film for different dyes. The Raman spectra for various dyes (1×10^{-8} M) on NC-NbSe₂ films, including indocyanine green (ICG), methylene blue (MB), 2-(4-Amidinophenyl)-6-indolecarbamide dihydrochloride (DAPI).

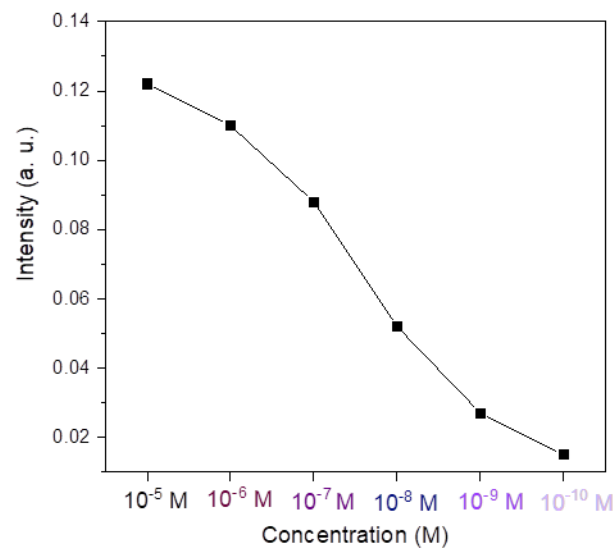


Figure S9. The SERS effect of as-grown NC-NbSe₂ film as a function of dye concentrations. Raman intensity at 1361 cm⁻¹ as a function of R6G concentrations.

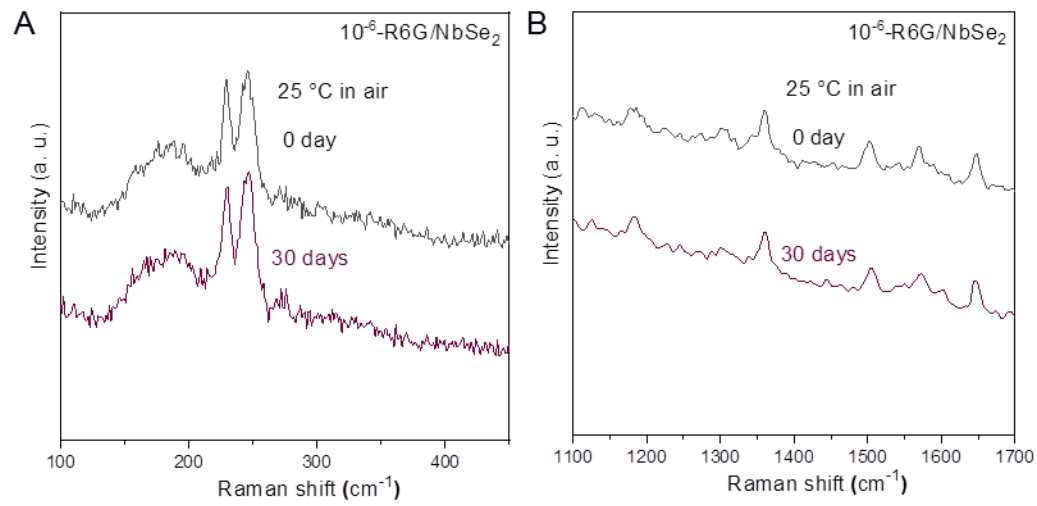


Figure S10. Air-stable SERS effect of as-grown NC-NbSe₂ film. The Raman spectra of (A) NC-NbSe₂ films and (B) coated R6G molecules before/after exposure to air for 30 days at 25 °C.

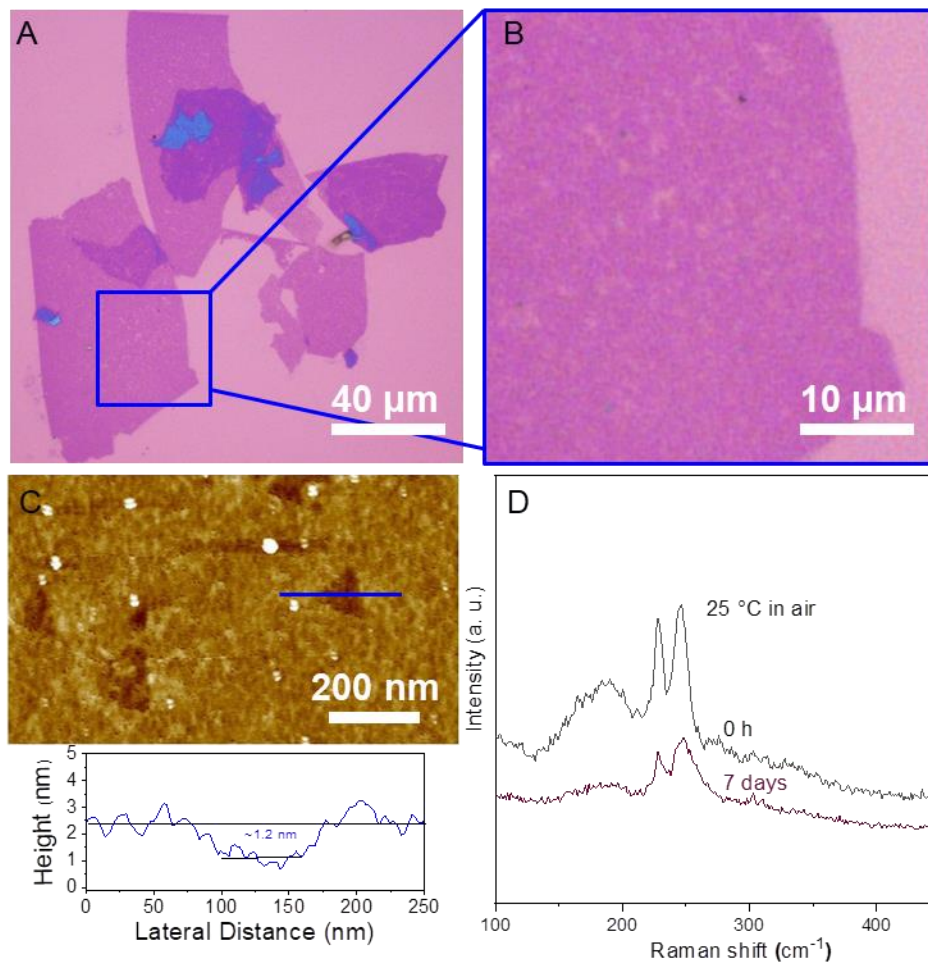


Figure S11. Instability of electrochemically exfoliated NbSe₂ flakes. (A, B) The optical images, (C) AFM image and the corresponding height profile, and (D) Raman spectra of electrochemically exfoliated NbSe₂ after exposure to air at 25 °C 7 days.

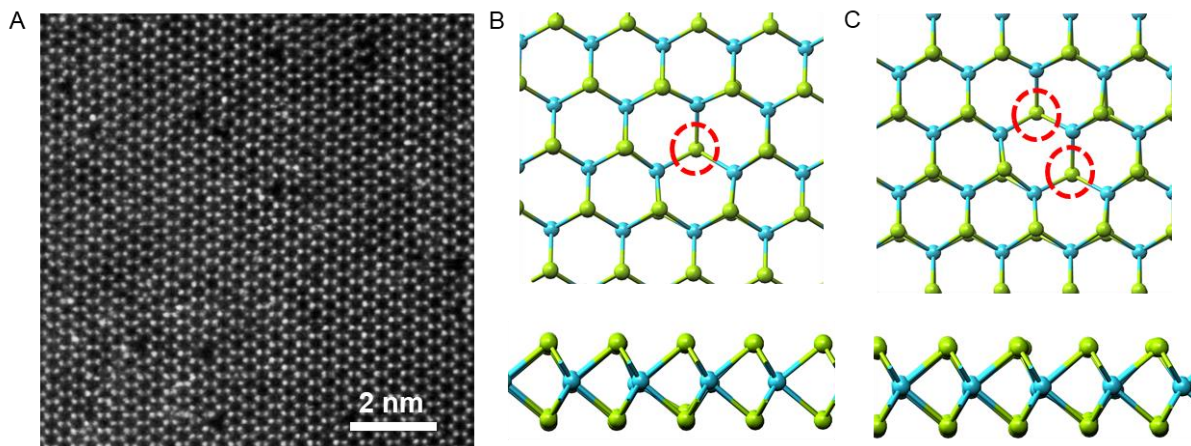


Figure S12. Origin of instability in electrochemically exfoliated NbSe₂ flakes. (A) ADF-STEM images of monolayer NbSe₂ after an exposure to air for few minutes. B, the sites of single Se vacancy and double Se vacancies created in monolayer NbSe₂ atomic model structures.

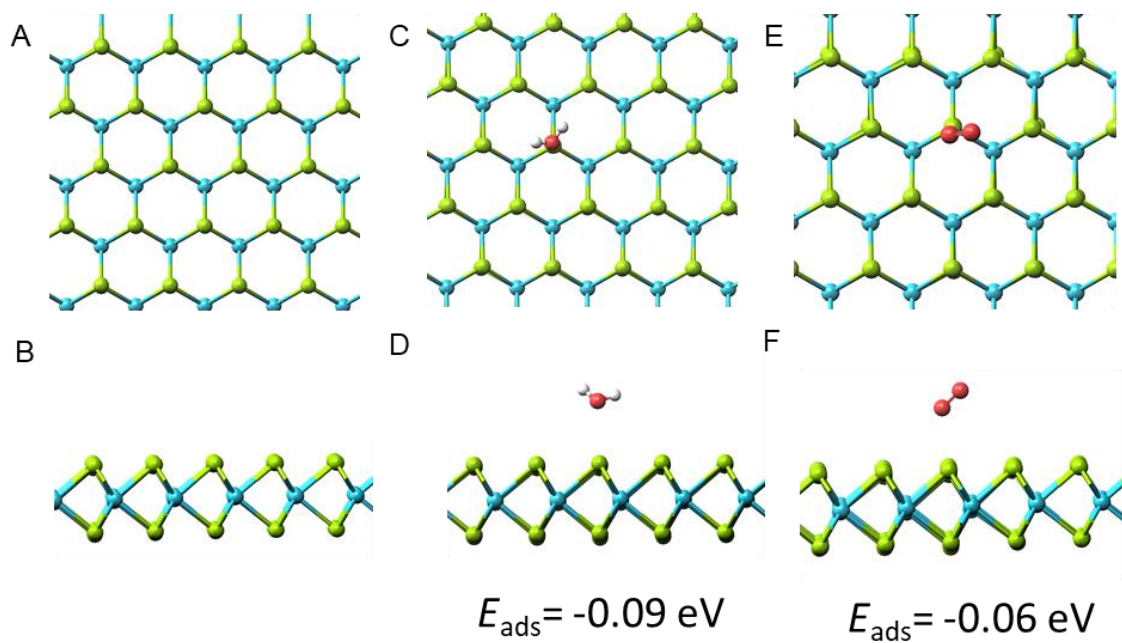


Figure S13. Pristine NbSe₂ flakes in air. Side-view and top-view of atomic model structures of (A, B) defect-free monolayer NbSe₂. (C, D) H₂O adsorbed on defect-free monolayer NbSe₂, (E, F) O₂ adsorbed on defect-free monolayer NbSe₂.

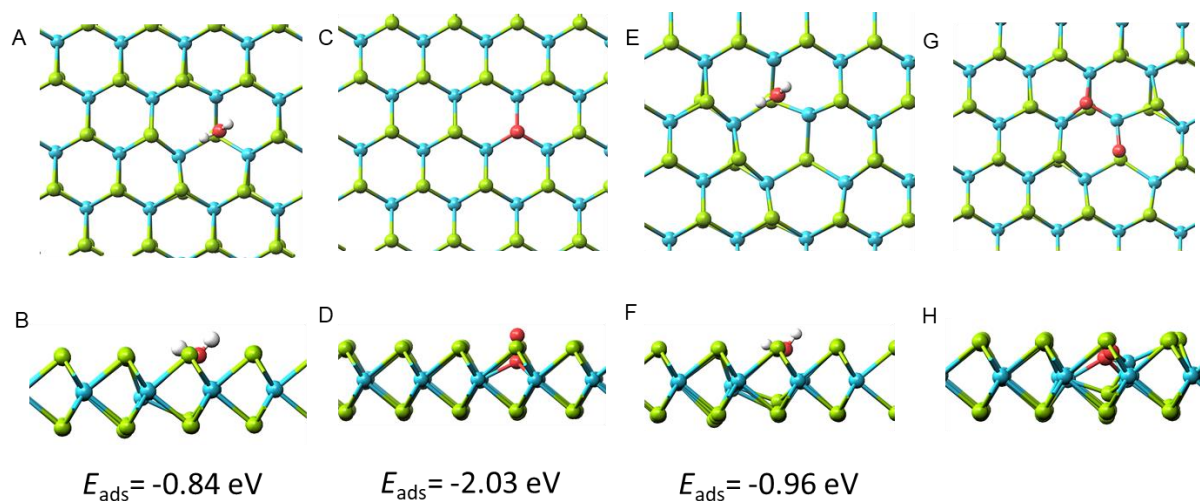


Figure S14. NbSe₂ flakes with points defect in air. Side-view and top-view of atomic model structures of H₂O (A, B) and O₂ (C,D) adsorbed on single Se vacancy of monolayer NbSe₂. Side-view and top-view of atomic model structures of H₂O (E, F) and O₂ (G, H) adsorbed on dual Se vacancies of monolayer NbSe₂. Note: No E_{ads} in case of O₂ (G, H) adsorbed on dual Se vacancies of monolayer NbSe₂, due to O₂ is directly dissociated and be embedded in NbSe₂.

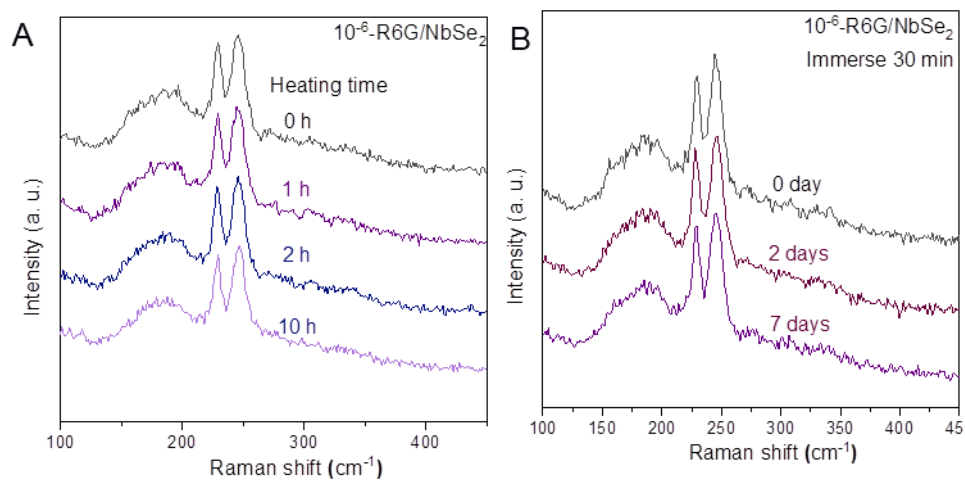


Figure S15. Stable SERS effect of NC-NbSe₂ film. (A) The time-dependent evolution of Raman spectra of NC-NbSe₂ films exposure to air at 50 °C. (B) The time-dependent evolution of Raman spectra NbSe₂ films after being pre-immersed in water for 30 minutes.

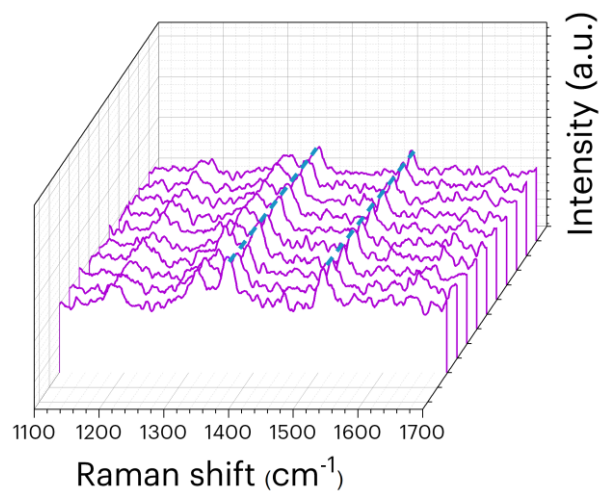


Figure S16. Homogenous SERS performance of as-grown 4-inch NC-NbSe₂ film. Raman spectra at 10 different locations randomly distributed in the 10⁻⁶ M R6G coated 4-inch as-grown NC-NbSe₂ film.

Table 1: Comparative Analysis with representative 2D SERS Substrates.

Catalysts	Dyes	Detect Limit (M)	Stability	Refs.
Graphene quantum dots	R6G	1×10^{-9}	/	Nature Communications, 2018, 9, 193-202.[1]
1T'-W(Mo)Te ₂	R6G	1×10^{-15}	Stable in air with 12 days	<i>J. Am. Chem. Soc.</i> , 2018, 140, 8696-8704.[2]
NbS ₂	MB	1×10^{-14}	Stable in air with 3 days	ACS Nano 2019, 13, 8312-8319.[3]
6L NbSe ₂	R6G	1×10^{-16}	Unstable SERS in air	<i>J. Mater. Chem. A</i> , 2021, 9, 2725-2733.[4]
TaSe ₂ Film	R6G	1×10^{-10}	/	<i>Small</i> 2022, 18, 2107027.[5]
NC-NbSe ₂	R6G	1×10^{-10}	Stable with 7 days after pre-treatment in water 30 min/ Stable in air with 30 days	This work